High-Performance Sensor Fault-Tolerant Control Based on μ-Synthesis Approach for Induction Motor

Samira Benaicha, Hadda Benderradji

University Batna2, Department of Electrical Engineering, LSPIE Laboratory
05000 Batna, Algeria, e-mail: samira.benaicha@univ-batna2.dz ,
h.benderradji@univ-batna2.dz

Abstract: In this paper, we present an improved Fault-Tolerant Control (FTC) for an Induction Motor (IM) system associated with a robust sensor Fault Detection and Isolation (FDI) filter based on the robust μ-synthesis technique. The proposed approach is founded on the implementation of two robust regulators and a performance indicator obtained using robust analysis tools (the structured singular value μ). The FTC is configured by switching between these two regulators, one ensures IM operation for a multiplicative fault and the other for additive faults. The indicator permits the extraction of the optimal FDI/FTC pair for a given application and set of specifications. Simulations of the FDI and FTC schemes of the induction motor are given to verify the effectiveness of the proposed method.

Keywords: Induction motor; field-oriented control; robust control; μ-synthesis; fault-tolerant control; fault detection and isolation; sensors

1 Introduction

Various industrial applications of induction motor torque and speed drives require extremely strict specifications where static and dynamic performance must be very high, which necessitates an advanced robust control algorithm [1]. One of the most popular control strategies for IMs is the Field-Oriented Control (FOC) technique [2]. However, the performance of this technique is still influenced by uncertainties, which are usually composed of external load disturbances, parameter variations, and unmodeled dynamics, particularly when classical PI(Proportional-Integrator) controllers are used. To overcome these constraints, several advanced control techniques have been developed. Robust control methods, such as Sliding Mode Control (SMC) [3] and H-infinity control(H∞) [4], [5] are frequently employed to improve system resilience in the face of uncertainty. Alternatively, adaptive strategies that optimize PI gains in real-time have gained popularity[6-8], including Gain Scheduling PI Controllers [9], as well as intelligent control techniques such as

fuzzy logic, neural networks and genetic algorithms, [10]. All the mentioned techniques have their advantages and disadvantages to address the issue of robustness.

The H-infinity control strategy appears to be a promising solution to these problems [5]. An extension to the H∞ optimal control technique known as μ-synthesis controlwasintroduced in the early 1980s by [11] to provide a general framework for solving the problem of robustness analysis in the presence of uncertainties and disturbances [11], [12].The stability margin in front of a perturbation is typically obtained by calculating the structured singular value (μ).

In addition to the problems already mentioned, high-performance FOC induction motor drives depend primarily on the quality of feedback information from sensors [1], [13]. Nevertheless, this control method requires the speed sensor to correctly determine the orientation of the rotor flux vector. A faulty speed sensor causes significant performance degradation and even instability in the system. Consequently, it is important to design a class of controllers to compensate for fault effects and guarantee system stability with acceptable performance. This type of control strategy is called the Fault-Tolerant Control System (FTC) [13-14].

The FTC is characterized by its ability to maintain acceptable performance of control systems under different situations, including nominal and faulty conditions. A fault-tolerant control system can automatically accommodate faults that may affect its various components [14]. The FTC methods can be classified into two types, namely passive and active approaches[15]. In the passive approach, the controller is based on robust control theory and ensures that the closed-loop system remains insensitive to the occurrence of certain faults. Reliable control techniques [16]are also included in the passive approach. In the case of an active approach, the objective is to ensure the control systems when faults occur through accommodation and control reconfiguration[13], [15]. In this context, a fault detection and isolation (FDI) algorithm has a very important role in control reconfiguration. FDI methods can be classified into two main categories: signal-based and model-based strategies [13]. Model-based FDI strategy has a wider range of applications than signal-based FDI and consists of two steps: residual generation and residual evaluation through a decision system[1], which has the role of determining if the residual is significant to decide whether a fault exists. However, the important problem that arises when synthesizing a model-based monitoring system is to guarantee residual robustness to uncertainties such as system deviation, disturbances, and unknown nonlinearities. Thereby,achieving a high detection rate with a lower false alarm rate and to separate between default effects and the effects of uncertain signals and disturbances. Several approaches of fault-tolerant control applied to differentelectrical systems have been proposed in the literature [16-18].

Encoder speed feedback is critical for torque regulation in induction motors that apply the field-oriented control strategy. When speed sensor faults occur, they must be detected and corrected quickly to ensure consistent performance. The concept of

a fault-tolerant sensor has garnered significant attention in recent times. In [19], a logic-based method compares measured or reference speed to estimated value using stator currents in a vector-controlled IM drive. [20] employs state augmentation and system transformation to decouple sensor fault variables and achieve fault-tolerant control. In [21], the authors developed a diagnostic algorithm using sliding mode observers and current spectral analysis to identify sensor and induction motor faults. [22] describes a FDI strategy based on a Takagi-Sugeno (T-S) fuzzy model that provides reliable fault estimation. Although these methods reduce fault effects, they often neglect issues related to parameter variations and external disturbance, especially in decoupling faults from perturbations in residual signals despite the use of robust techniques like T-S fuzzy and sliding mode control.

To address speed sensor faults with the problems mentioned, [23] suggests two active FTC schemes. The first is a hybrid control system with a PI controller under nominal conditions and an H∞ loop-shaping controller activated upon fault detection through residual signal analysis. The second is a generalized internal model control (GIMC) scheme that allows for natural reconfiguration. The hybrid approach suffers from transients and poor dynamics during fault-induced switching, whereas the GIMC provides better transition performance. However, neither approach considers the impact of parameter changes or load disturbance. To improve robustness, [24] proposes a scheme that includes three speed controllers and a voting algorithm. This algorithm selects the most appropriate controller output and functions as an implicit FDI mechanism, increasing fault tolerance in the presence of parameter uncertainties and sensor faults.

Controllers based H∞ also offer good performance in both steady-state and transient operations, even in the presence of parameter variations and disturbances. For this reason, in this work, we chose to use the extended H∞ control (μ-synthesis) to develop a fault-tolerant control strategy for IM based on robust fault estimation and compensation of sensor speed faults for an induction motor. The main idea in this work is to use a reconfiguration control law mechanism to accommodate speed sensor faults and to maintain tracking performance by using two robust controllers and a μ-synthesis filter. In comparison to [23-24], the following are the main contributions in this paper:

In [23-44],the authors used a PI controller in normal operation. In the present work, a robust mu-synthesis control is used against parameter variations, load torque disturbances, and multiplicative faults. As a result, the nominal control is robust and able to operate in the presence of multiplicative faults without activation of the FTC control.

To design μ-synthesis controllers, the parameters of weighing functions are adjusted by the algorithm proposed in [25] to overcome all IM control situations (normal or faulty), as opposed to [23], where these parameters are fixed.

In [24], authors propose a complex FDI structure because the voting algorithm needs information from the inputs of the speed sensor and two observers (virtual

sensors) to decide between the three controllers. In our work, the FDI used a robust filter capable of detecting and decoupling faults and disturbances to avoid false alarms.

Following the introduction, this work is organized as follows: The proposed fault-tolerant strategy is described in Section 2. In Section 3, the IM direct rotor field orientation control is presented. A brief description of μ-synthesis theory is offered in Section 4. Two robust speed controllers for faulty situations are developed in Section 5. In Section 6, an H∞ descriptor fault detection filter-based μ-synthesis is formulated. Simulation and results are reported in Section 7, and conclusion is given in Section 8.

2 Robust Fault Tolerant Structure

The proposed active fault-tolerant control system only considers speed sensor faults, which can degrade overall performance and stability. The main parts of this FTC structure are:

- Reconfigurable control consists of two robust speed controllers based on the μ-synthesis approach: $K_{\mu1}(s)$ is designed for structured uncertainties and multiplicative faults, and $K_{\mu2}(s)$ is considered for active missions and attenuation of constraints.
- Robust fault detection and isolation unit: it focuses on developing an efficient FDI system to detect and isolate sensor faults, generate alarm signals, and reconfigure the control law to maintain stability and performance by switching between $K_{\mu1}(s)$ and $K_{\mu2}(s)$.
- A residue r_f delivered by the FDI unit serves as a fault indicator. Consequently, $K_{\mu2}(s)$ is activated only when an additive fault is detected and the residue exceeds certain limits (threshold th):

$$\begin{cases} if \|r_f\| < th & only\ K_{\mu1}(s)\ is\ actived \\ if \|r_f\| \geq th & only\ \ K_{\mu2}(s)\ is\ actived \end{cases} \quad (1)$$

The schematic diagram of the fault-tolerant control applied to the induction motor is illustrated in Fig. 1. In the following sections, each part of this block diagram will be developed.

3 Direct Rotor Field oriented IM Dynamic Model

The nonlinear induction motor model in a d-q synchronously rotating frame can be determined by the voltage and flux equations of the stator and rotor [1], [2]. The direct rotor field-oriented control (DR-FOC) design, only the rotor equations and the electromagnetic torque are exploited:

$$\begin{cases} \dot{\phi}_{rd} = \frac{L_m}{T_r} i_{sd} - \frac{1}{T_r}\phi_{rd} + \omega_{sl}\phi_{rq} \\ \dot{\phi}_{rq} = \frac{L_m}{T_r} i_{sq} - \frac{1}{T_r}\phi_{rq} - \omega_{sl}\phi_{rd} \\ \dot{\Omega} = \frac{n_p}{J}.\frac{L_m}{L_r}\left(\phi_{rd}.i_{sq} - \phi_{rq}i_{sd}\right) - \frac{f_v}{J}.\Omega - \frac{1}{J}T_l \end{cases} \quad (2)$$

where ϕ_{rd} and ϕ_{rq} are the -d and -q axis rotor fluxes; i_{sd} and i_{sq} are the -d and q-axis stator currents; R_r is the rotor resistance; L_r and L_m are the rotor self-inductance and mutual inductance; $T_r = L_r/R_r$ is the rotor time constant; n_p is the pole-pairs number; J is the inertia moment; f_v is the friction coefficient; T_l is load torque considered as an unknown disturbance; ω_s, ω_r and $\omega_{sl} = \omega_s - \omega_r$ are the synchronous, rotor and slip angular speed, $\Omega = \omega_r/n_p$ is the mechanical speed.

The rotor field-oriented control of an induction motor requires that the rotor flux vector $[\phi_{rd}, \phi_{rq}]^t$ is forced on the d-axis ($\phi_{rq} = 0$, $\phi_{rd} = \phi_r$) , where ϕ_r must track the reference rotor flux ϕ_r^* [2].

To achieve the classical DR-FOC control objective, two conventional PI controllers are applied to control speed and rotor flux. In this work, the speed controller type PI is replaced by the robust controller ($K_{\mu 1}(s)$ or $K_{\mu 2}(s)$). The DR-FOC is not robust against parameter variations and sensor faults, on the other hand. The frequency approach to μ-synthesis is a very interesting method to have acceptable performance in the presence of parameter variations and faults. In this work, only the rotor speed loop is used to build the proposed FTC.

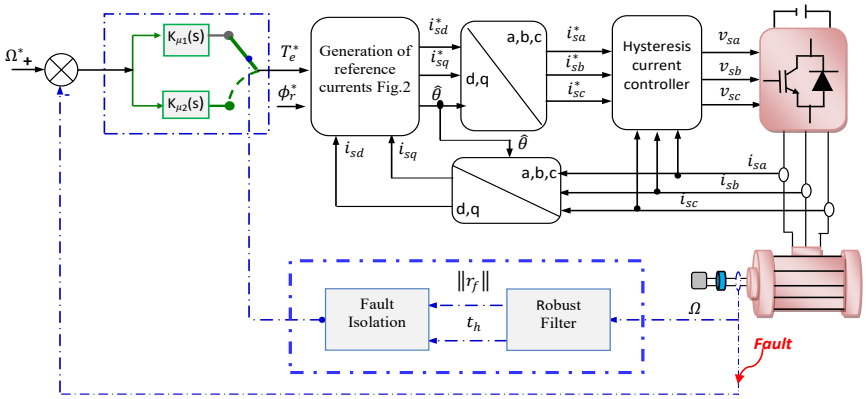

Figure 1
Structure of the proposed robust active FTC control of the induction motor

4 Speed Controller-based μ-synthesis Technique

Both robust controllers of rotor speed ($K_{\mu1}(s)$ and $K_{\mu2}(s)$) based on the μ-synthesis technique, using the D-K iteration algorithm, are developed to design and assure reconfigurable robust sensor fault-tolerant control of induction motor (see Fig. 2).

Next, each regulator $K_{\mu1}(s)$ and $K_{\mu2}(s)$ is synthesized and designed independently.

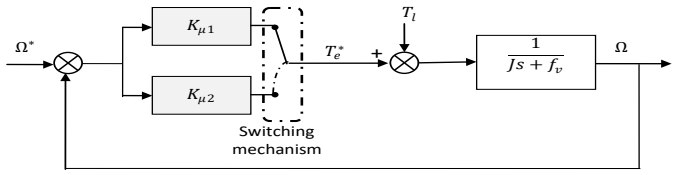

Figure 2
Reconfigurable rotor speed loop

4.1 Robust Speed Controller against Multiplicative Faults

A robust speed controller$K_{\mu1}(s)$ via μ-synthesis technique to guarantee closed-loop stability and performance under uncertain parameters, unknown disturbance (load torque) and the time delay is designed in Fig. 3.

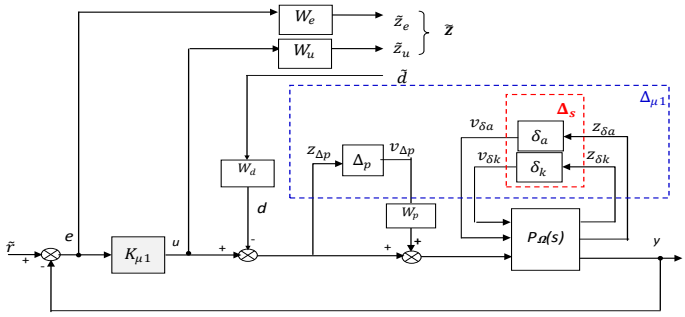

Figure 3
Closed-loop interconnection structure for $K_{\mu1}(s)$ controller

where, $\tilde{r} = \Omega^*$ is the reference input, $\tilde{d} = T_l$ is the unknown disturbance, $\tilde{Z} = [\tilde{z}_e \quad \tilde{z}_u]^t$ is the output vector of the interconnection matrix, $e = \Omega^* - \Omega$ is the input of controller (error speed), $u = T_e^*$ is output of controller (the torque reference) and $y = \Omega$ is output signal. W_e, W_u and W_d are weighting functions used to shape the closed loop system responses according to the robust performance and stability margin requirements. $P_\Omega(s)$denotes the nominal open-loop interconnected transfer function. $\Delta_s(s)$is the structured uncertainties bloc, (we limit our analysis to mechanical parameters: coefficient of friction and inertia moment, the electrical parameters are assumed to be known). $\Delta_p(s)$ is the unstructured uncertainty bloc.

The closed-loop interconnected structure in Fig. 3 is represented in general standard block diagram of a robust control in Fig. 4a, where $\Delta_{\mu 1} = \mathrm{diag}(\Delta_p, \ \Delta_s)$. To ensure that the designed controller achieves robust performance, we introduce a fictitious uncertainty block Δ_F as shown in Fig. 4b.

$P_{\mu 1}(s)$ is the nominal open-loop interconnected transfer function matrix, which includes the nominal system model and weighting functions,with input vector $[\mathrm{v}_{\Delta p} \ \ \mathrm{v}_{\delta k} \ \ \mathrm{v}_{\delta a} \ \ \tilde{\mathrm{r}} \ \ \tilde{\mathrm{d}} \ \ \mathrm{u}]^{\mathrm{t}}$ and output vector $[\mathrm{z}_{\Delta p} \ \ \mathrm{z}_{\delta k} \ \ \mathrm{z}_{\delta a} \ \ \tilde{\mathrm{z}}_{\mathrm{e}} \ \ \tilde{\mathrm{z}}_{\mathrm{u}} \ \ \mathrm{e}, y]^{\mathrm{t}}$:

$$P_{\mu 1}(s) = \begin{bmatrix} 0 & 0 & 0 & 0 & -W_d & 1 \\ W_p & 0 & 0 & 0 & W_d & 1 \\ W_p G & G & G & 0 & -W_d G & G \\ -W_e W_p G & -W_e G & -W_e G & W_e & W_e W_d G & -W_e G \\ 0 & 0 & 0 & 0 & 0 & W_u \\ -W_p G & -G & -G & 1 & W_d G & G \\ W_p G & 0 & 0 & 0 & -W_d G & G \end{bmatrix} \tag{3}$$

$P_{\mu 1}(s)$ is the nominal open-loop interconnected transfer function matrix, which includes the nominal system model and weighting functions, with input vector $[\mathrm{v}_{\Delta p} \ \ \mathrm{v}_{\delta k} \ \ \mathrm{v}_{\delta a} \ \ \tilde{\mathrm{r}} \ \ \tilde{\mathrm{d}} \ \ \mathrm{u}]^{\mathrm{t}}$ and output vector $[\mathrm{z}_{\Delta p} \ \ \mathrm{z}_{\delta k} \ \ \mathrm{z}_{\delta a} \ \ \tilde{\mathrm{z}}_{\mathrm{e}} \ \ \tilde{\mathrm{z}}_{\mathrm{u}} \ \ \mathrm{e}, y]^{\mathrm{t}}$ is given by equation (13).

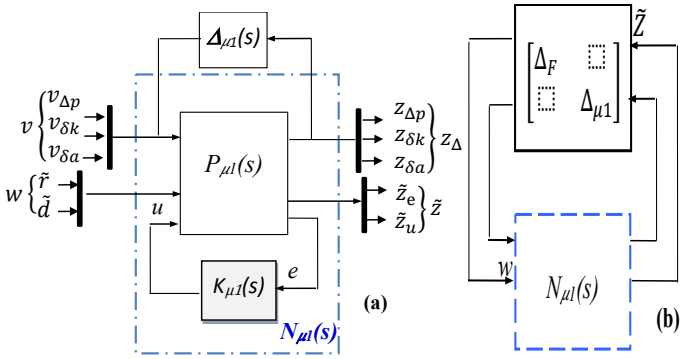

Figure 4
Standard N-Δ configuration for μ-synthesis

$$P_{\mu 1}(s) = \begin{bmatrix} 0 & 0 & 0 & 0 & -W_d & 1 \\ W_p & 0 & 0 & 0 & W_d & 1 \\ W_p G & G & G & 0 & -W_d G & G \\ -W_e W_p G & -W_e G & -W_e G & W_e & W_e W_d G & -W_e G \\ 0 & 0 & 0 & 0 & 0 & W_u \\ -W_p G & -G & -G & 1 & W_d G & G \\ W_p G & 0 & 0 & 0 & -W_d G & G \end{bmatrix} \tag{4}$$

The close loop system $\mathrm{N}_{\mu 1}(\mathrm{s})$ is defined by:

$$N_{\mu 1}(s)\begin{bmatrix} -W_p T_{\Delta\mu 1} & -T_{\Delta\mu 1} & -T_{\Delta\mu 1} & K_{\mu 1} S_{\Delta\mu 1} & W_d T_{\Delta\mu 1} \\ W_p S_{\Delta\mu 1} & -T_{\Delta\mu 1} & -T_{\Delta\mu 1} & K_{\mu 1} S_{\Delta\mu 1} & -W_d S_{\Delta\mu 1} \\ W_p S_{\Delta\mu 1} G & G S_{\Delta\mu 1} & G S_{\Delta\mu 1} & T_{\Delta\mu 1} & W_d G S_{\Delta\mu 1} \\ -W_e G S_{\Delta\mu 1} W_p & -W_e G S_{\Delta\mu 1} & -W_e G S_{\Delta\mu 1} & -W_e S_{\Delta\mu 1} & W_e G S_{\Delta\mu 1} W_d \\ W_u T_{\Delta\mu 1} W_d & -W_u T_{\Delta\mu 1} & -W_u T_{\Delta\mu 1} & W_u K_{\mu 1} S_{\Delta\mu 1} & W_u T_{\Delta\mu 1} W_d \end{bmatrix} \quad (5)$$

4.1.1. Structured Uncertainties of IM

Structured uncertainties $\Delta_s(s)$ are determined via interval bound by unknown parameters [5]. The open-loop transfer function of induction motor speed is given by:

$$G(s) = \frac{k}{s+a} \quad (6)$$

where, $k = \frac{1}{J}$ and $a = \frac{f_v}{J}$.

The uncertainties in the "k" and "a" parameters are represented by following expressions:

$$\begin{cases} k = k_0(1 + e_k \delta_k) \\ a = a_0(1 + e_a \delta_a) \end{cases} \quad (7)$$

k_0 and a_0 are the nominal values for the parameters "k" and "a". Values e_k and e_a represent the percentages of variation around the nominal values and δ_k, δ_a are the normalized uncertainty variable such that: $|\delta_k| < 1 \text{and} |\delta_a| < 1$.

The following diagonal matrix represents structured uncertainties.

$$\Delta_s(s) = \begin{bmatrix} \delta_k & 0 \\ 0 & \delta_a \end{bmatrix} \quad (8)$$

4.1.2 Unstructured Uncertainties of IM

Unstructured uncertainties $\Delta_p(s)$ are used to model the system's dynamic perturbation, such as unmodelled high-frequency dynamics and they are available in two forms: additive and/or multiplicative [12]. The neglect time delay can be interpreted as a multiplicative uncertainty, as shown in:

$$G_\Omega(s) = G(s)e^{\tau' s} = G(s)\big(1 + W_p(s)\Delta_p(s)\big) \quad (9)$$

where, $G_\Omega(s)$ represents an uncertain model, G(s) is a nominal model and $W_p(s)$ is the upper bound of the multiplicative uncertainty deduces by using the first-order "Padé-approximation"[5]:

$$W_p(s) = \frac{\tau_m \cdot s}{1 + \tau_m \cdot s/2}; \qquad |\Delta_p| < 1 \quad (10)$$

where, τ_m is the maximum neglect delay time.

Finally, the uncertainty matrix can be written as follows:

$$\Delta_{\mu 1}(s) = \begin{bmatrix} \delta_k & 0 & 0 \\ 0 & \delta_a & 0 \\ 0 & 0 & \Delta_p \end{bmatrix} \tag{11}$$

In terms of the (N-Δ) structure in Fig. 4, the requirements for stability and performance (SP) can be guaranteed via theorem given by [26]. Consequently, to achieve robust performance (RP), the stabilizing controller $K_{\mu 1}(s)$ should minimize using equation. (10):

$$max_{\omega \in \mathbb{R}} \mu_{\underline{\Delta}} \left| N_{\mu 1}(j\omega) \right| < 1 \tag{12}$$

The criteria (12) cannot be definite except if the nominal performance condition is proved and the following performance criterion is satisfied:

$$\left\| \begin{matrix} W_e(s).S_{\Delta\mu 1} & -W_e(s).G.S_{\Delta\mu 1}.W_d(s) \\ W_u(s).K_{\mu 1}.S_{\Delta\mu 1} & W_u(s).T_{\Delta\mu 1}.W_d(s) \end{matrix} \right\| < 1 \tag{13}$$

Where, $(S_{\Delta\mu 1}(s))$ and $(T_{\Delta\mu 1}(s))$ are the sensitivity and complementary sensitivity functions respectively for the nominal system defined as follows:

$$\begin{cases} S_{\Delta\mu 1}(s) = 1/\left(1 + K_{\mu 1}(s)G(s)\right) \\ T_{\Delta\mu 1}(s) = K_{\mu 1}(s)G(s)/\left(1 + K_{\mu 1}(s)G(s)\right) \end{cases} \tag{14}$$

4.2 Robust Speed Controller against Multiplicative and Additive Faults

The closed-loop interconnection structureof the $K_{\mu 2}$ controller is shown by Fig. 5, which considers faulty conditions, external disturbances and model uncertainties and can take the similar standard (N-Δ) configuration of Fig. 4, where Δ_{mf} presents a multiplicative faults matrix:

$$\Delta_{mf}(s) = \begin{bmatrix} \delta_{kf} & 0 \\ 0 & \delta_{af} \end{bmatrix} \tag{15}$$

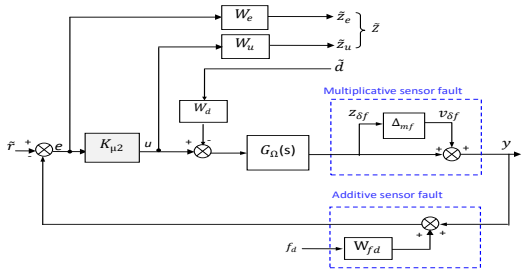

Closed-loop interconnection structure for $K_{\mu 2}(s)$ controller

The nominal open-loop $P_{\mu 2}(s)$determined by equations (16) and (17)

$$P_{\mu 2}(s)=\begin{bmatrix} 0 & 0 & 0 & 0 & -W_d & 0 & 1 \\ W_p & 0 & 0 & 0 & -W_d & 0 & 1 \\ W_pG & G & G & 0 & -W_dG & 0 & G \\ -W_pW_eG & -W_eG & -W_eG & W_e & W_dW_eG & -W_eW_{fd} & -W_eG \\ 0 & 0 & 0 & 0 & 0 & 0 & W_u \\ -W_pG & -G & -G & 1 & -W_dG & -W_{fd} & -G \\ W_pG & G & G & 0 & -W_dG & 0 & G \end{bmatrix} \quad (16)$$

The lower linear fractional transformation $N_{\mu 2}(s)$ is given by:

$$N_{\mu 2}(s) = \begin{bmatrix} -W_pT_{\Delta\mu 2} & -T_{\Delta\mu 2} & -T_{\Delta\mu 2} & K_{\mu 2}S_{\Delta\mu 2} & -S_{\Delta\mu 2}.W_d & K_{\mu 2}S_{\Delta\mu 2}W_{fd} \\ W_pS_{\Delta\mu 2} & -T_{\Delta\mu 2} & -T_{\Delta\mu 2} & K_{\mu 2}S_{\Delta\mu 1} & -S_{\Delta\mu 2}W_d & -K_{\mu 2}S_{\Delta\mu 2}W_{fd} \\ GS_{\Delta\mu 2} & GS_{\Delta\mu 2} & GS_{\Delta\mu 2} & T_{\Delta\mu 2} & -GS_{\Delta\mu 2}W_d & -T_{\Delta\mu 2}W_{fd} \\ -W_eGS_{\Delta\mu 2}W_p & -W_eGS_{\Delta\mu 2} & -W_eGS_{\Delta\mu 2} & W_eS_{\Delta\mu 2} & W_eGS_{\Delta\mu 2}W_d & -W_eS_{\Delta\mu 2}W_{fd} \\ -W_uT_{\Delta\mu 2}W_d & -W_uT_{\Delta\mu 2} & -W_uT_{\Delta\mu 2} & W_uK_{\mu 2}S_{\Delta\mu 2} & W_uT_{\Delta\mu 2}W_d & -W_uK_{\mu 2}S_{\Delta\mu 2}W_{fd} \end{bmatrix} \quad (17)$$

The desired conditions of nominal performance are well achieved if the following condition is satisfied:

$$\left\| \begin{matrix} W_e(s).S_{\Delta\mu 2} & W_e(s).G.S_{\Delta\mu 2}.W_d(s) & -W_e(s).S_{\Delta\mu 2}.W_{fd}(s) \\ W_u(s).K_{\mu 2}.S_{\Delta\mu 2} & W_u(s).T_{\Delta\mu 2}.W_d(s) & -W_u(s).K_{\mu 2}.S_{\Delta\mu 2}.W_{fd}(s) \end{matrix} \right\| < 1 \quad (19)$$

Weighting functions selection is a critical step in the development of robust μ-synthesis -synthesis control in order to attain the robust performance objectives of both controllers $K_{\mu 1}(s)$, and $K_{\mu 2}(s)$.

5 Weighting Functions Selection

The choice of weighting functions and the closed-loop system design specifications are mutually dependent. These functions have a physical interpretation that is associated with the desired closed-loop behavior, according to Fig. 4 and Fig. 6 and to achieve robust and stability performance of the induction motor, weighting functions should be properly selected in advance in order to find both controllers $K_{\mu 1}(s)$ and $K_{\mu 2}(s)$. The weight W_e is usually selected to get disturbance rejection, good tracking and zero steady state error, W_u is required to prevent the saturation of controller output, the weighting function, W_d is used to scale external disturbances and W_{fd} is chosen to achieve the system robustness objectives with respect to additive faults.The control problem is reduced to designing a controller that minimizes the weighted signals as much as possible. We can clearly see from criteria (13), (19) and properties of the norm H∞ stated in [5], that closed-loop sensitivity functions $S_{\Delta\mu 1,2}$, $KS_{\Delta\mu 1,2}$, $GS_{\Delta\mu 1,2}$ and $T_{\Delta\mu 1,2}$ are constrained by

desirable templates. Consequently, checking specifications is equivalent to testing conditions (13) and (19).

Weighting functions of various types (gain, first order, etc.) can be selected and provide general guidelines for selecting the most suitable weight functions as given in [27], [28]. In this paper, the choice of weighting functions is given by:

$$\begin{cases} W_e(s) = \frac{1}{M_e}.\frac{s+\omega_e.M_e}{s+\omega_e.\varepsilon_e} \\ W_u(s) = \frac{s+\frac{\omega_u}{M_u}}{\varepsilon_u s+\omega_u.} \\ W_d(s) = \beta_d \\ W_{fd}(s) = \beta_{fd} \end{cases} \tag{20}$$

where, M_e is an upper bound for the peak sensitivity ε_e is a low-frequency tracking error specification and ω_e is approximately the bandwidth requirement. M_u and ω_u reflect the limited gain and bandwidth of the actuator and ε_u is a property influenced by the sensor noise characteristics.

5.1 Adaptation to the Weighting Functions Parameters

The D-K iteration is performed for a variety of weighting functions that provide an appropriate balance between robustness and system performance. In the majority of studies, the selection of these weights is founded on the method proposed in [27], [28] and the final selection weighting parameters are often the result after a long process of trial and error. The main disadvantage of this approach is that when system model parameters change or a fault occurs, the desired robustness level and detection performance are not achieved, consequently, weights must be readjusted. An automatic weighting function selection algorithm suggested in [25] is used in this work to optimize these weights by introducing judiciously weighted function parameters. It is an iterative algorithm using initial weighting functions that reflect the desired performance specifications. The objective of this algorithm is to adjust the weighting function parameters until the various performance criteria specified in the robust control are satisfied. According to the robust stability and performance criteria, the algorithm detects a minimum structured singular value (μ) to have an appropriate response.

The initial parameter weighting functions are determined by:

$$\begin{cases} W_e(s) = \frac{0.3326.s+3.952}{s+0.01875} \\ W_u(s) = \frac{8.10^5 s+9.032.10^6}{s+1.875.10^8} \\ W_d(s) = 0.31 \\ W_{fd}(s) = 0.01 \end{cases} \tag{21}$$

$K_{\mu1}(s)$ and $K_{\mu2}(s)$ are optimized by D-K iteration using the "dksyn" Matlab function and reduced to 3rd order via Hankel-Norm approximation with reasonable stability margins, as shown in Table 1.

Table.1
Stability margins obtained by robust regulators $K_{\mu1}(s)$ and $K_{\mu2}(s)$

	Phase margin	Gain margin
$K_{\mu2}(s)$	66.8°	44.4 dB
$K_{\mu2}(s)$	66.5°	31 dB

$K_{\mu1}(s)$ and $K_{\mu2}(s)$ are given by:

$$K_{\mu1}(s) = \frac{15{,}84\ s^2+116\ s+2{,}573}{s^3+88{,}16s^2+3{,}604\ s+0{,}03654} \quad (22)$$

$$K_{\mu2}(s) = \frac{8{,}478\ s^2+7{,}833.10^4 s+5{,}761.10^5}{s^3+890{,}5\ s^2+2{,}834.10^5 s+5305} \quad (23)$$

At low, medium, and high frequencies, Figs. 6 and 7 show how the selected templates influence the different transfer functions. The desired conditions of nominal performance (13) and(19) are achieved. The sensibility functionsshow a very low gain, which implies perfect tracking (error ≈0) and good disturbance rejection. $T_{\Delta\mu1,2}$ have a very low gain at high frequencies, which give very good attenuation of multiplicative faults. $K_{\mu1,2}S_{\Delta\mu1,2}$ are not constrained at low frequencies, but a constraint is imposed at high frequencies. The upper bound on $GS_{\Delta\mu1,2}$ closely resembles the objectives imposed by filters W_eW_d and W_{fd}

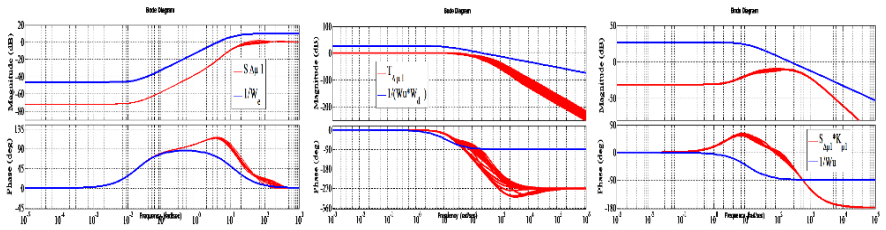

Figure 6
Minimization of sensitivity functions ($S\Delta_{\mu1}$, $T\Delta_{\mu1}$ and $S\Delta_{\mu1}.K\Delta_{\mu1}$) in Case of regulator $K_{\mu1}$

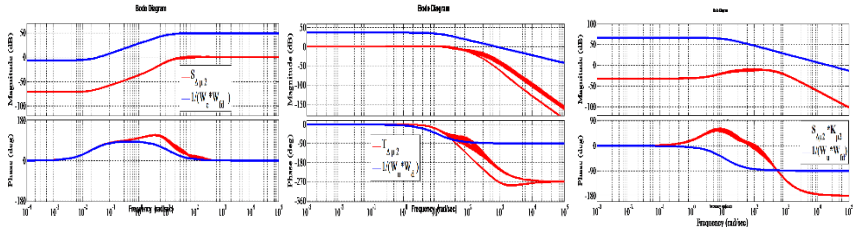

Figure 7
Minimization of sensitivity functions ($S\Delta_{\mu2}$, $T\Delta_{\mu2}$ and $S\Delta_{\mu2}.K\Delta_{\mu2}$) in Case of regulator $K_{\mu2}$

6 Fault Detection and Isolation (FDI)

Model-based FDI methods require a mathematical model representing the behavior of the system. However, an accurate and exact model of a real system cannot be obtained. This can be caused by a number of factors, including an unknown disturbance structure, various noise effects, and uncertain variables. The term "robustness residue" refers to FDI methods that can account for model uncertainty of this type [13]. As a result, the residue is a fault detection signal that corresponds to the difference between the nominal system model and the fault model. The fault estimation can be taken as residue. In order to detect the moment when a fault appears, this residue must be compared to detection thresholds. Model uncertainty can cause either false alarms or missed alarms, therefore, this uncertainty must be taken into account when performing the FDI. In this paper, a robust diagnostic filter synthesis method is designed using the approach of μ-synthesis.

7.1 μ-synthesis Fault Detection Filter Design

The design of a robust fault detection filter is typically an optimization problem with the following maximization criterion [29]:

$$\bar{J}_{opt} = \frac{\left\| T_{f_d - r_f}(j\omega) \right\|_\infty}{\left\| T_{d - r_f}(j\omega) \right\|_\infty} \tag{24}$$

The robust problem is equivalent to the H∞ norm minimization problem: $\min\left\|T_{d-r_f}(j\omega)\right\|_\infty$ and the requirement for robust fault sensitivity can be expressed as the criterion: $\max\left\|T_{f_{d-r_f}}(j\omega)\right\|_\infty$.

where, T_{d-r_f} is the transfer function from the disturbance to the residual r_f and $T_{f_d-r_f}$ the transfer function from the default to the residual. We can also define the estimation fault $\hat{f}_d$. The difference between f_d and $\hat{f}_d$, is denoted by z_f.. The FDI filter synthesis problem is described by an augmented model represented in Fig. 11a.

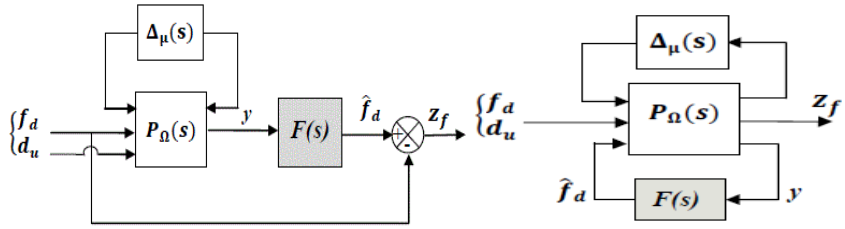

Figure 8
Scheme of the FDI filter and standard form using the H_∞/μ-synthesis

The residual signal $r_f(s)$ considered in this paper has the following form and was proposed by [30]:

$$r_f(s) = H_y(s).y(s) + H_u(s).u(s) \tag{25}$$

According to equation (25), H_y and H_u take the following forms [29], [30]:

$$\begin{cases} H_y(s) = F(s) \\ H_u(s) = F(s).G_u(s) \end{cases} \tag{26}$$

$G_u(s)$ is the transfer function from input u(t) to output y(t).

The objective is to realize a robust filter F(s) with a fault indicator that is only sensitive tofaults. F(s) is synthesized to maximize the smallest singular value of the transfer function between f_d and $\hat{r}_f$ (sensitivity constraint) and to minimize the greatest singular value of the transfer function between d and $\hat{r}_f$ (robustness constraint). Preferably, the residual should be zero in healthy operating conditions and significant in the presence of a fault.FDI filter using H_∞/μ-synthesis (Fig. 8a) can take the same standard form of μ-synthesis problem as Fig. 4, which is illustrated in Fig. 8b.

Hence, the augmented model of interconnect diagram is defined as follows:

$$P(s) = F_l\left((P_\Omega s), \Delta_\mu(s)\right) = \begin{bmatrix} 1 & 0 & -1 \\ G_{f_{d-\Delta}}(s) & G_{d-\Delta}(s) & 0 \end{bmatrix} \tag{27}$$

$G_{f_{d-\Delta}}(s)$ and $G_{d-\Delta}(s)$ are uncertain functions. The obtained FDI filter is given by the flowing expression:

$$F(s) = \frac{4{,}76.10^2}{108{,}2\ s^2+678{,}6\ s+131{,}9} \tag{28}$$

8 Simulation Results

In order to validate the proposed FTC strategy performance shown in Fig. 1, simulations have been carried out for an induction motor using MATLAB/Simulink; two different tests are considered. Parameters induction motor of 5 (kW), 220 (V) and 7.5 (A) are: R_s=1.78 (Ω), R_r =1.68 (Ω), L_s=0.295 (H), L_r=0.104 (H), Lm=0.165 (H), J=0.01 (Kg. m^2), f_v=0.00027 (Nm s rad^{-1}).

8.1 Test 1: Performance of $K_{\mu 1}(s)$ and $K_{\mu 2}(s$

In this test, the FDI mechanism is not connected; only the DR-FOC control is used. This study compares the performance of $K_{\mu 1}(s)$ and $K_{\mu 2}(s)$ controllers to identify their respective advantages and disadvantages. Both controllers' responses are observed under a variety of operating conditions, including a step change in load

torque and faulty conditions. The rotor speed is fixed at 1450 (rpm). Figs. 9 and 10 show simulation results for $K_{\mu 1}(s)$ and $K_{\mu 1}(s)$.

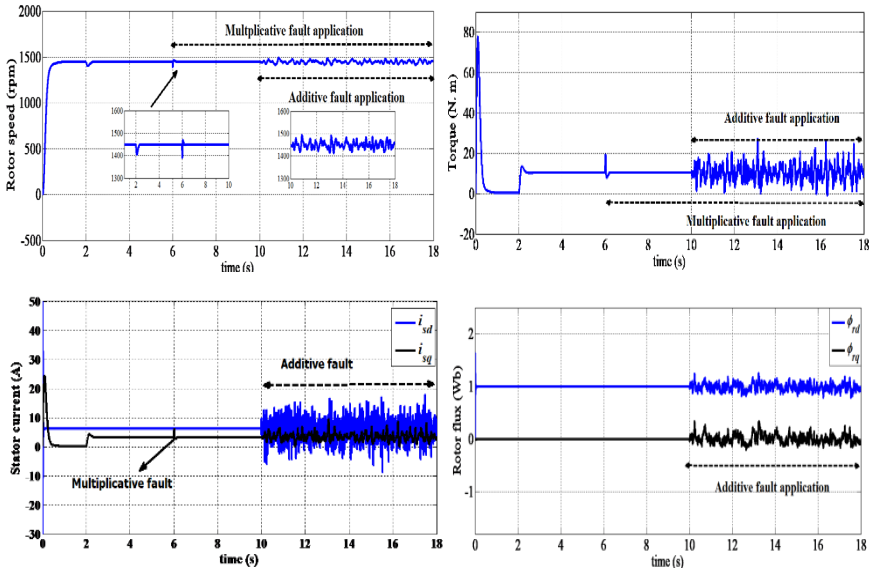

Figure 9
Test 1 performance of DR-FOC control $K_{\mu 1}$

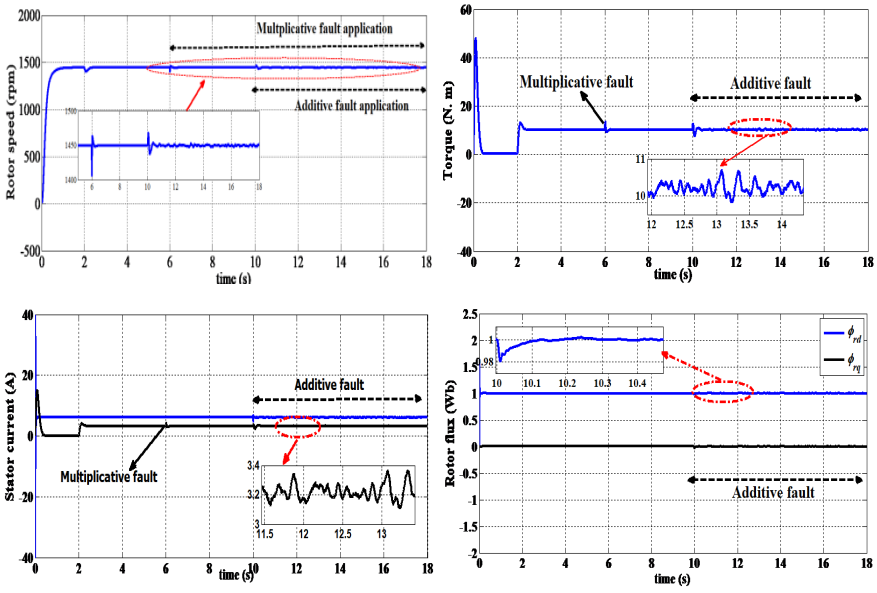

Figure 10
Test 1 performance of DR-FOC control $K_{\mu 2}$

A rated load torque is applied at t = 1 s, followed by a multiplicative fault (variation of J and f_v) at t = 5 s, and finally an additive fault (noise speed sensor) is introduced at t = 10 s. We can observe:

- When a multiplicative fault was applied, the reaction to this fault in both controllers is rejected.
- DR-FOC is not robust during the application of an additive fault at t =10 s when $K_{\mu 1}(s)$ is used, but it is robust in the case of controller $K_{\mu 2}(s)$.

8.2 Test 2: Performances of Proposed FTC

In order to prove effectiveness and robustness of the proposed FTC, the operating conditions have been specified by:

- The reference speed and rotor flux are maintained at rated speed (1450 rpm) and 1Wb respectively with load torque applied at 1 s.
- An abrupt variation of mechanical parameters ($J = J_0 + 20\% J_0$ and $f_v = f_{v0} + 30\%. f_{v0}$) is applied (multiplicative fault) at 6 s.
- A speed sensor noise N (0, 10) (0: mean and σ=10 rad/s=95.5 (rpm) is the variance) is introduced as an additive fault at t=10 s.
- The switching between $K_{\mu 1}(s)$ and $K_{\mu 2}(s)$ is delayed for 2 s at 10 s ≤ t <12 s (at 12 s the $K_{\mu 2}(s)$ is activated).
- A threshold is selected at th=0.15 to avoid false alarms. To extract the useful residual signal, a low-pass filter (LPF) is used.

The plot Fig. 11a presents the estimated fault, and Fig. 11b depicts the residual without and with LPF. The residual has excellent robustness to external disturbances (load torque), a multiplicative fault, and high sensitivity to an additive sensor fault.

The results presented in Fig. 12 show the effectiveness of the suggested FTC method against multiplicative and additive sensor faults. In the first part (0 ≤ t <12 s), only the controller $K_{\mu 1}$ is activated. A multiplicative speed sensor fault appears at t=6 s, we can see that the speed, the electromagnetic torque, the two components of stator current, and the two components of rotor flux are unaffected, but after the additive fault appears at t=10 s, high ripples appear in these signals. As a result, at t=12 s, the information issued by the FDI block is used by the FTC reconfiguration control law to compensate the fault. In the second part (12 s≤ t <18 s), $K_{\mu 2}$ is activated to reduce the effect of the fault by eliminating ripples.

Simulation results show clearly that the proposed active fault-tolerant control using mu-synthesis provides highly satisfactory performances in terms of robustness against noise (harmonics reduction), disturbance (load torque), system uncertainty, and parameter variations. We can notice that the residue is insensitive in the

presence of multiplicative faults and disturbances Fig. 1 (the residual error is approximately zero). Results have confirmed the effectiveness of the robust residual error generation fault detection based μ-synthesis.

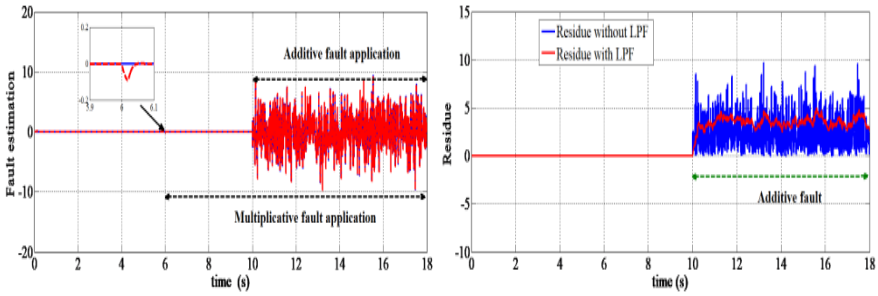

(a) (b)

Figure 11

Fault estimation and residue evaluation

Simulation results show clearly that the proposed active fault-tolerant control using mu-synthesis provides highly satisfactory performances in terms of robustness against noise (harmonics reduction), disturbance (load torque), system uncertainty, and parameter variations. We can notice that the residue is insensitive in the presence of multiplicative faults and disturbances Fig. 1 (the residual error is approximately zero). Results have confirmed the effectiveness of the robust residual error generation fault detection based μ-synthesis.

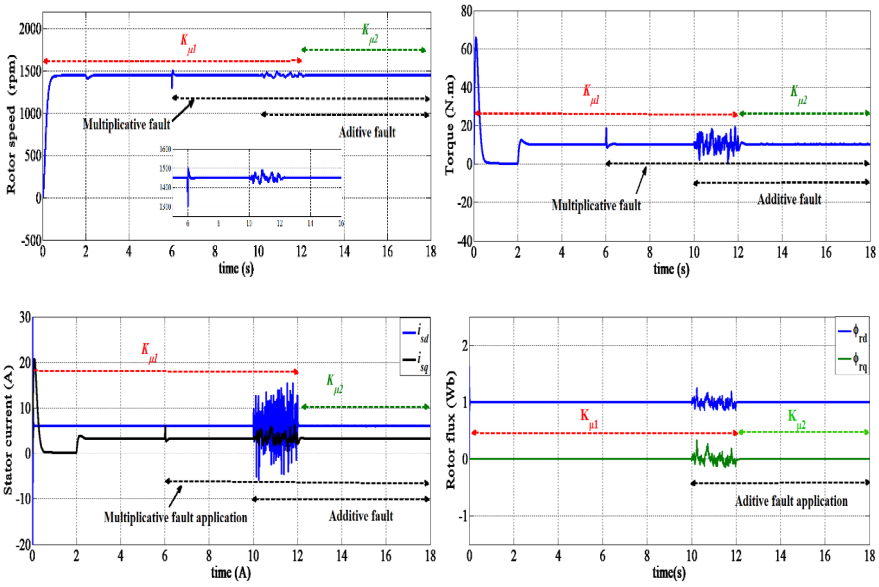

Figure 12

FTC performance in the presence of speed sensor faults

Simulation results show clearly that the proposed active fault-tolerant control using mu-synthesis provides highly satisfactory performances in terms of robustness against noise (harmonics reduction), disturbance (load torque), system uncertainty, and parameter variations. We can notice that the residue is insensitive in the presence of multiplicative faults and disturbances Fig. 1 (the residual error is approximately zero). Results have confirmed the effectiveness of the robust residual error generation fault detection based μ-synthesis.

Conclusions

In this paper, a robust fault-tolerant control for IM based on a robust FDI diagnostic filter ensuring operation with acceptable performance is presented. The proposed FTC approach is based on the H∞/μ-synthesis technique in order to eliminate the effect of speed sensor faults. Therefore, we can conclude that the frequency method μ-synthesis allowed us to synthesize a robust FDI diagnostic filter tolerating an approximate decoupling of the exogenous residue disturbance and sensitizing only to the fault in additive form.Thus, offering a robust active FTC control configurable law that admits a means of transition between two robust controllers: Simulation results show that the proposed algorithm can successfully detect, isolate, and identify sensor faults in the presence of perturbations and uncertainties.

References

[1] F. Giri: Electric Motors Control: Advanced Design Techniques and Applications, John Wiley & Sons. Nashville, TN, 2013

[2] F. Blaschke: The Principle of Field Orientation as Applied to the New Transvector Closed Loop Control System in a PWM Inverter Induction Motor Drive, Siemens Review, Vol. 34, 1972, pp. 217-222

[3] A. A. Hagras, A. Azab, S. Zaid: Model-Free Nonsingular Fast Terminal Sliding Mode Control of a Permanent Magnet Synchronous Motor, ACTA Polytechnica Hungarica, Vol. 21(11), 2024, pp. 283-305

[4] K. Yeneneh M. Walle, T. Mamo, Y. Yalew: Optimizing Active Suspension Systems with Robust H∞ Control and Adaptive Techniques under Uncertainties", Applications in Engineering Science, 2025, p. 100225

[5] P. Feyel: Robust Control Optimization with Metaheuristics, John Wiley & Sons, New York, 2017

[6] R. C. Roman, R. E. Precup, S. Preitl, A. I. Szedlak-Stinean, C. A. Bojan-Dragos, E. M. Petriu: PI controller Tuning Via Data-Driven Algorithms for Shape Memory Alloy Systems, IFAC-PapersOnLine, Vol. 55(40), 2022, pp. 181-186

[7] I. A. Zamfirache, R. E. Precup, E. M. Petriu: Adaptive Reinforcement Learning-Based Control Using Proximal Policy Optimization and Slime Mould Algorithm with Experimental Tower Crane System Validation, Applied Soft Computing, Vol. 160, 2024, p. 111687

[8] Á. Takács, L. Kovács, I. Rudas, R. E. Precup, T. Haidegger: Models for Force Control in Telesurgical Robot Systems, ACTA Polytechnica Hungarica, Vol. 12(8), 2015, pp. 95-114

[9] J. Han, X. Shan, H. Liu, J. Xiao, T. Huang: Fuzzy Gain Scheduling PID Control of a Hybrid Robot Based on Dynamic Characteristics, Mechanism and Machine Theory, Vol. 184, 2023, pp. 105283

[10] V. Chopra, S. K. Singla, L. Dewan: Comparative Analysis of Tuning a PID Controller Using Intelligent Methods, ACTA Polytechnica Hungarica, Vol. 11(8), 2014, pp. 235-249

[11] M. G. Safonov, J. C. Doyle: Minimizing Conservativeness of Robustness Singular Values, In: Tzafestas, S.G. (eds) Multivariable Control: New Concepts and Tools, Springer, Dordrecht, 1984, pp.197-207

[12] T. Roy, R. K. Barai: Robust Control-Oriented Linear Fractional Transform Modelling, Spinger nature, 2023

[13] S. X. Ding: Advanced Methods for Fault Diagnosis and Fault-Tolerant Control, Berlin, Germany: Springer, 2021

[14] Y. Zhang, J. Jiang: Bibliographical Review on Reconfigurable Fault-Tolerant Control Systems", Annual reviews in control, Vol. 32(2), 2008, pp. 229-252

[15] J. Jiang, X. Yu: Fault-Tolerant Control Systems: A Comparative Study Between Active and Passive Approaches, Annual Reviews in control, Vol. 36(1), 2012, pp. 60-72

[16] L. Timilsina, P. R. Badr, A. Arsalan, G. Ozkan, B. Papari, C.S. Edrington: Reliable Fault-tolerant Distributed Control for Traction IPMSM in Electric Vehicle/Hybrid Electric Vehicle, IEEE Transportation Electrification Conference and Expo (ITEC), 2024, pp. 1-6

[17] M. S. S. Chandra, S. Mohapatro: Sensor Fault Tolerant Control in Modern and Green Power Applications: A Review; IEEE Transactions on Instrumentation and Measurement, Vol. 73, 2024, pp. 1-24

[18] W. Lee, G. Choi: A Comprehensive Review of Fault-Tolerant AC Machine Drive Topologies: Inverter, Control, and Electric Machine, IEEE 13th International Symposium on Diagnostics for Electrical Machines, Power Electronics and Drives, Vol. 1, 2021, pp. 269-275

[19] M. Dybkowski, K. Klimkowski, and T. Orłowska-Kowalska: Speed and Current Sensor Fault-Tolerant-Control of the Induction Motor Drive",. In Advanced Control of Electrical Drives and Power Electronic Converters, Cham: Springer International Publishing, 2016, pp. 141-167

[20] S. Xu, J. Wang, H. Chai, Y. Chai, W. Xing Zheng: A Simultaneous Detection and Tolerant Control Method for Current- and Speed-Sensor Faults in

Induction Motor, In IEEE Transactions on Instrumentation and Measurement, Vol. 74, 2025, pp. 1-12

[21] A. Gouichiche, A. Safa, A. Chibani, and M. Tadjine: Global Fault-Tolerant Control Approach for Vector Control of an Induction Motor, International Transactions on Electrical Energy Systems, Vol. 30(8), 2020, p. e12440

[22] H. B. Zina, M. Allouche, M. Bouattour, M. Souissi, A. Chaabane, M., L. Chrifi-Alaoui: Robust fuzzy fault tolerant control for induction motor subject to sensor fault. International Journal of Automation and Control, Vol. 12(2), 2018, pp. 271-290

[23] A. Raisemche M. Boukhnifer, C. Larouci, and D: Two Active Fault-Tolerant Control Schemes of Induction-Motor Drive in EV or HEV, IEEE Transactions on Vehicular Technology, Vol. 63(1), 2013, pp. 19-29

[24] A. Raisemche, M. Boukhnifer, D. Diallo: New Fault-Tolerant Control architectures based on Voting Algorithms for Electric Vehicle Induction-Motor Drive, Transactions of the Institute of Measurement and Control, Vol. 38(9), 2016, pp. 1120-1135

[25] S. S Nair: Automatic Weight Selection Algorithm for Designing H-Infinity Controller for Active Magnetic Bearing, International Journal of Engineering Science and Technology, Vol. 3(1), 2001, pp. 122-38

[26] J. C. Doyle: Structured Uncertainty in Control System design, IEEE 24th IEEE Conference on Decision and Control - Fort Lauderdale, FL, USA 1985, pp. 260-265

[27] D. Pathak, D. K. Sambariya: Methodologies for the Selection of Weighting Function, 2nd International Conference on Power Energy, Environment and Intelligent Control (PEEIC), Greater Noida, India, October 2019, pp. 347-350

[28] L. Pettazzi, A. Lanzon: Systematic Design of Optimal Performance Weight and Controller in Mixed-μ Synthesis, IFAC Proceedings, Vol. 41(2), 2008, pp. 7814-7819

[29] A. Farhat, D. Koenig: Robust Fault Detection for Uncertain Switched Systems, IFAC-Papers Online, Vol. 50(1), 2017, pp. 15265-15270

[30] J. Chen: Formulating and Solving Robust Fault Diagnosis Problems Based on a H∞ Setting, IFAC Proceedings, Vol. 41(2), 2008, pp. 7259-7264